Building anisotropic models

Dave Nichols

ABSTRACT

The elastic properties of layered and fractured anisotropic media can be calculated using the group theoretic approach of Schoenberg and Muir. I present a computational toolkit for calculating these properties from the properties of the constituent rocks . The toolkit is used to build a model with laterally varying anisotropy. Synthetic data produced by finite difference elastic modeling demonstrates the effects of this type of anisotropy.

INTRODUCTION

Recent developments in modeling elastic waves in general anisotropic media (Etgen 1987) have made it practical to consider routine generation of synthetic multi-component seismograms. However in specifying an elastic model it is necessary to provide many more parameters than with acoustic models. To model an axially symmetric medium (transverse isotropy) 4 stiffness coefficients and the density must be specified, to model a general anisotropic medium all 21 stiffness coefficients and the density must be specified. A method is required to generate these parameters for geologically 'reasonable' models.

Schoenberg and Muir (1988) have presented a method for calculating the effective elastic constants for a geologic unit consisting of many finely bedded layers of anisotropic rocks. They also show how to calculate the elastic constants for fractured media as a limiting case of very fine, very compliant layers. The only limitation on this method is that the scale of the layering in any geologic unit must be much finer than the wavelength of the seismic energy. This is the 'quasistatic' assumption.

A model may be built up of many such heterogeneous rock units and the relative amounts of the component rocks in any unit may vary laterally. This paper describes a computational toolkit for building anisotropic models and shows one example model and the synthetic two component dataset created.

A REVIEW OF THEORY

The method used is that outlined by Muir in SEP–56 and more fully described by Schoenberg and Muir (1988) and Muir (1988). The calculation of the properties of layered media is related to the work of Backus (1962) and gives the equivalent elastic properties of a layered medium for layering much finer than the seismic wavelength.

Hooke's law for a general elastic medium can be written as,

$$\begin{bmatrix} \sigma_1 \\ \sigma_2 \\ \sigma_3 \\ \sigma_4 \\ \sigma_5 \\ \sigma_6 \end{bmatrix} = \begin{bmatrix} c_{11} & c_{12} & c_{13} & c_{14} & c_{15} & c_{16} \\ c_{21} & c_{22} & c_{23} & c_{24} & c_{25} & c_{26} \\ c_{31} & c_{32} & c_{33} & c_{34} & c_{35} & c_{36} \\ c_{41} & c_{42} & c_{43} & c_{44} & c_{45} & c_{46} \\ c_{51} & c_{52} & c_{53} & c_{54} & c_{55} & c_{56} \\ c_{61} & c_{62} & c_{63} & c_{64} & c_{65} & c_{66} \end{bmatrix} \begin{bmatrix} \epsilon_1 \\ \epsilon_2 \\ \epsilon_3 \\ \epsilon_4 \\ \epsilon_5 \\ \epsilon_6 \end{bmatrix}$$

where

$$\begin{bmatrix} \sigma_1 \\ \sigma_2 \\ \sigma_3 \\ \sigma_4 \\ \sigma_5 \\ \sigma_6 \end{bmatrix} = \begin{bmatrix} \sigma_{11} \\ \sigma_{22} \\ \sigma_{33} \\ \sigma_{23} \\ \sigma_{31} \\ \sigma_{12} \end{bmatrix} \quad \textit{and} \quad \begin{bmatrix} \epsilon_1 \\ \epsilon_2 \\ \epsilon_3 \\ \epsilon_4 \\ \epsilon_5 \\ \epsilon_6 \end{bmatrix} = \begin{bmatrix} \epsilon_{11} \\ \epsilon_{22} \\ \epsilon_{33} \\ 2\epsilon_{23} \\ 2\epsilon_{31} \\ 2\epsilon_{12} \end{bmatrix} .$$

are the stress and strain tensors written in the abbreviated subscript notation.

Schoenberg and Muir (1988) and Muir (SEP–57) show that if the following 3×3 matrices are defined for the i^{th} component of a layered medium,

$$\mathbf{C}_{NN_i} = \begin{bmatrix} c_{11_i} & c_{12_i} & c_{16_i} \\ c_{12_i} & c_{22_i} & c_{26_i} \\ c_{16_i} & c_{26_i} & c_{66_i} \end{bmatrix} , \quad \mathbf{C}_{TT_i} = \begin{bmatrix} c_{33_i} & c_{34_i} & c_{35_i} \\ c_{34_i} & c_{44_i} & c_{45_i} \\ c_{35_i} & c_{45_i} & c_{55_i} \end{bmatrix} , \quad \mathbf{C}_{NT_i} = \begin{bmatrix} c_{13_i} & c_{14_i} & c_{15_i} \\ c_{23_i} & c_{24_i} & c_{25_i} \\ c_{36_i} & c_{46_i} & c_{56_i} \end{bmatrix} ,$$

and the thickness of all layers of the i^{th} constituent in the composite is H_i and its density is ρ_i, we can define the following transformation to 'group' coordinates,

$\mathbf{G}_i = [\, g_i(1), g_i(2), \mathbf{g}_i(3), \mathbf{g}_i(4), \mathbf{g}_i(5) \,]$ of two scalars and three 3×3 matrices.

The mapping is given by

$$\begin{bmatrix} H_i \\ H_i\,\rho_i \\ H_i\,\mathbf{C}_{TT_i}^{-1} \\ H_i\,\mathbf{C}_{NT_i}\,\mathbf{C}_{TT_i}^{-1} \\ H_i\,[\,\mathbf{C}_{NN_i} - \mathbf{C}_{NT_i}\mathbf{C}_{TT_i}^{-1}\mathbf{C}_{NT_i}^{T}\,] \end{bmatrix} \rightarrow \begin{bmatrix} g_i(1) \\ g_i(2) \\ \mathbf{g}_i(3) \\ \mathbf{g}_i(4) \\ \mathbf{g}_i(5) \end{bmatrix},$$

For any $\mathbf{G}_i$ such that $\mathbf{g}_i(1) \neq 0$ and $\mathbf{g}_i(3)$ is invertible, we can return to the set of physical model parameters by the 'inverse group mapping' from group element $\mathbf{G}_i$ to physical model. This inverse mapping is given by

$$\begin{bmatrix} g_i(1) \\ g_i(2)/g_i(1) \\ g_i(1)\mathbf{g}_i(3)^{-1} \\ \mathbf{g}_i(4)\mathbf{g}_i(3)^{-1} \\ [\mathbf{g}_i(5) + \mathbf{g}_i(4)\mathbf{g}_i(3)^{-1}\mathbf{g}_i(4)^{T}]/g_i(1) \end{bmatrix} \rightarrow \begin{bmatrix} H_i \\ \rho_i \\ \mathbf{C}_{TT_i} \\ \mathbf{C}_{NT_i} \\ \mathbf{C}_{NN_i} \end{bmatrix}.$$

The group has been chosen in this way in order that adding the respective scalars and matrices for all constituents of a layered composite and performing the inverse group transformation will give a set of elastic constants which is the long wavelength equivalent elastic medium.

The method of calculating the properties of fractured media is that described by Schoenberg and Douma (1988) which is shown by Schoenberg and Muir (1988) to correspond to increasing the third group element. A set of fractures is defined by a symmetric 3×3 matrix which is added to the third group element of the rock to be fractured.

A ROCK BUILDING TOOLKIT

A computing toolkit for modeling the elastic properties of rocks was developed. The toolkit enables the user to derive the elastic properties of layered and fractured media.

Description of toolkit functions

create Create a rock description by specifying the thickness density and the elastic constants or the P and S-wave velocities.

combine Combine two rock descriptions to create a single rock description with equivalent elastic properties to the finely layered heterogeneous rock and the appropriate thickness and density.

uncombine Subtract one rock description from another to create a new rock description.

crack Horizontally fracture a rock by adding a percentage of the third group element from one rock type to the rock. This adds fractures defined by the third group element of rock type A to rock B.

vcrack Vertically fracture a rock. This is achieved by rotating the elastic constants of the rock by 90 degrees about the y-axis , horizontally fracturing the rock and rotating the elastic constants by -90 degrees about the y-axis.

display Print the rock thickness, density and elastic constants and optionally the group form of the rock description.

laymod Create a model layer suitable for use in John Etgen's elastic finite difference modeling program. The user supplies the size of the model grid and two rock descriptions. The layer created grades uniformly from the rock described by the first set of parameters to the rock described by the second set. More complicated models may be created by combining the layers created by this program using the Seplib program Merge.

laymod21 Create a model layer suitable for use in Jean-Luc Guiziou's anisotropic ray tracing program, the output is all 21 independent elastic constants divided by density.

FOUR EXAMPLE ROCK TYPES

An isotropic rock

The rock description for an isotropic rock is created by specifying two elastic constants and the density. The elastic constants specified are c_{13} and c_{44} These two constants are the Lamé constants λ and μ . Alternatively the P-wave and S-wave velocities may be specified. An isotropic rock (called 'sst') created using the command
,

create sst c13=18.3E6 c44=7.68E6 rho=3 delz=1

will have the following properties : P-wave velocity 3000 m/s and S-wave velocity 1600 m/s . It could also be created using the command ,

create sst velp=3000. vels=1600. rho=3. delz=1 .

Figure 1 shows the group velocity surface for this rock. Since the rock is isotropic all the velocity surfaces are circles.

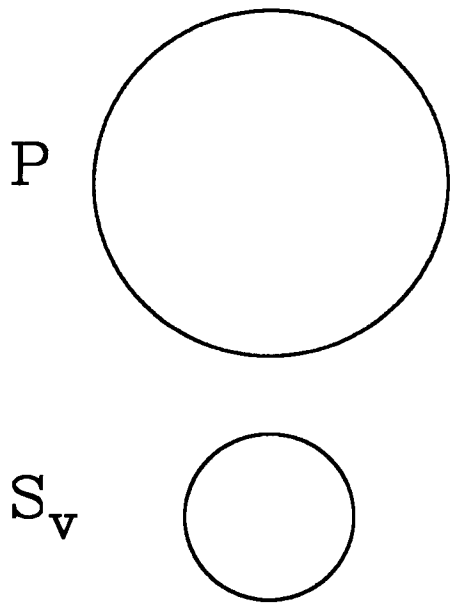

FIG. 1. Group velocity surfaces for rock 'sst'

A transversely isotropic rock

A transversely isotropic rock is created by specifying three or four elastic constants , if four are specified they are c_{13}, c_{12}, c_{44} and c_{66} if only three are specified they are c_{13}, c_{44}, and c_{66} , c_{12} is assumed to be the same as c_{13} . A transversely isotropic rock (called 'shl') created using the command ,

create shl c13=18.3E6 c44=7.68E6 c66=11.5092E6 rho=3 delz=1

will have the following properties : Vertical P-wave velocity 3000 m/s , vertically traveling Sv-wave 1600 m/s , horizontally traveling Sv-wave velocity 1920 m/s . This rock could also be created using the command,

create shl velp=3000. vels=1600. hvels=1920. rho=3. delz=1 .

Figure 2 shows the group velocity surfaces for this rock and the best fitting approximating ellipses. The best fitting ellipse corresponds the best fitting hyperbola in the T-X domain as discusses by Dellinger and Muir (1985). The fact that the best fitting ellipse for the P-wave surface has small ellipticity means that the velocity estimated by hyperbolic normal moveout scans will be the close to the true vertical velocity. The large ellipticity of the Sv-wave surface means that the velocity estimated by hyperbolic NMO scans will be much more than the true vertical velocity.

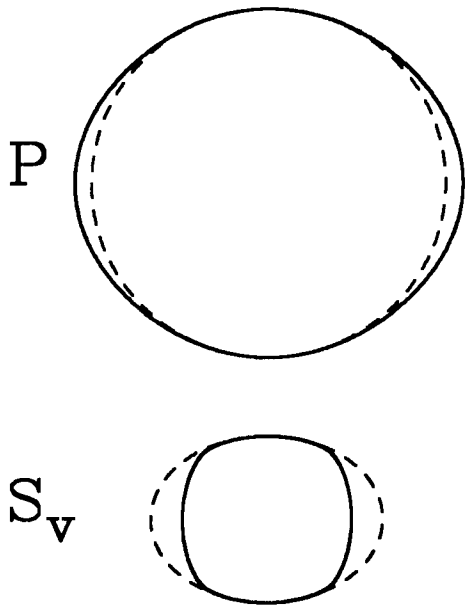

FIG. 2. Group velocity surfaces for rock 'shl' , the dashed line is the best fitting ellipse at small angles to the vertical

A layered rock

A rock consisting of layers of 'sst' of total thickness one and layers of 'shl' of total thickness one will have elastic constants given by the Schoenberg and Muir formulas provided that the thickness of the individual layers is well below the wavelength of the seismic energy. A rock (called 'mix') with such properties can be created using the command ,

combine shl sst mix .

Figure 3 shows the group velocity surfaces for this rock and the best fitting ellipses. The ellipticity is intermediate between that of the two constituent rocks 'sst' and 'shl'.

A vertically fractured rock

A vertically fractured rock is created by specifying the rock to be fractured and the rock whose third group element will be used to define the fractures. A fractured version of the rock 'shl' could be created using the command,

vcrack shl sst fracshl excess=10 .

This results in a new rock description 'fracshl' created by adding 10% of the third group element of the rock 'sst' to the third group element of the rock 'shl'. This will

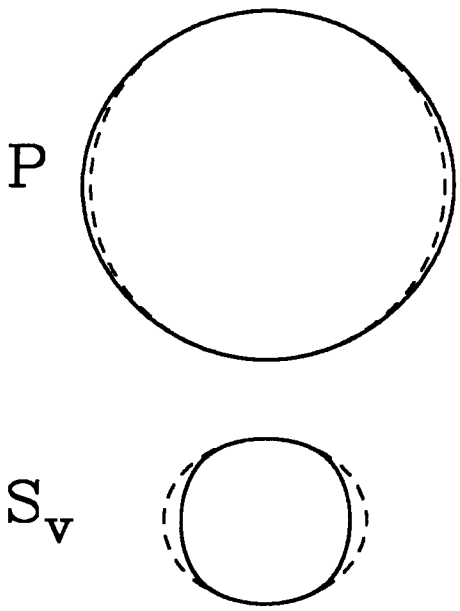

FIG. 3. Group velocity surfaces for rock 'mix'

produce a set of elastic parameters with orthorhombic symmetry. The symmetry plane is the X-Z plane (the plane of the fractures).

AN EXAMPLE MODEL

Building a model

A simple model was created to show some of the main effects observed when laterally varying anisotropy is encountered. The model is intended to represent a simple one layer section which is sandstone on the left and shale on the right with the two rocks interbedding in-between. The sandstone content changes from 100% , 1/4 of the way across the model to 0%, 3/4 of the way across the model. The standard way of depicting this would be as shown in figure 4 , this is a very misleading picture there are no large fingers of sandstone in the shale. The true picture is better depicted in figure 5 . The sandstone and shale are very finely interbedded with the transition from sandstone to shale in any one bed taking place fairly randomly at some point in the section, the overall effect is to make the percentage of sandstone below any surface point decrease uniformly from 1/4 to 3/4 of the across the section. The elastic properties of the sandstone and shale were those of the rocks 'sst' and 'shl' described earlier in this article. The two rocks were chosen to have the same vertical velocities for P-waves and S-waves. The zero offset travel times will therefore be the same for the whole model, but the hyperbolic NMO observed will change.

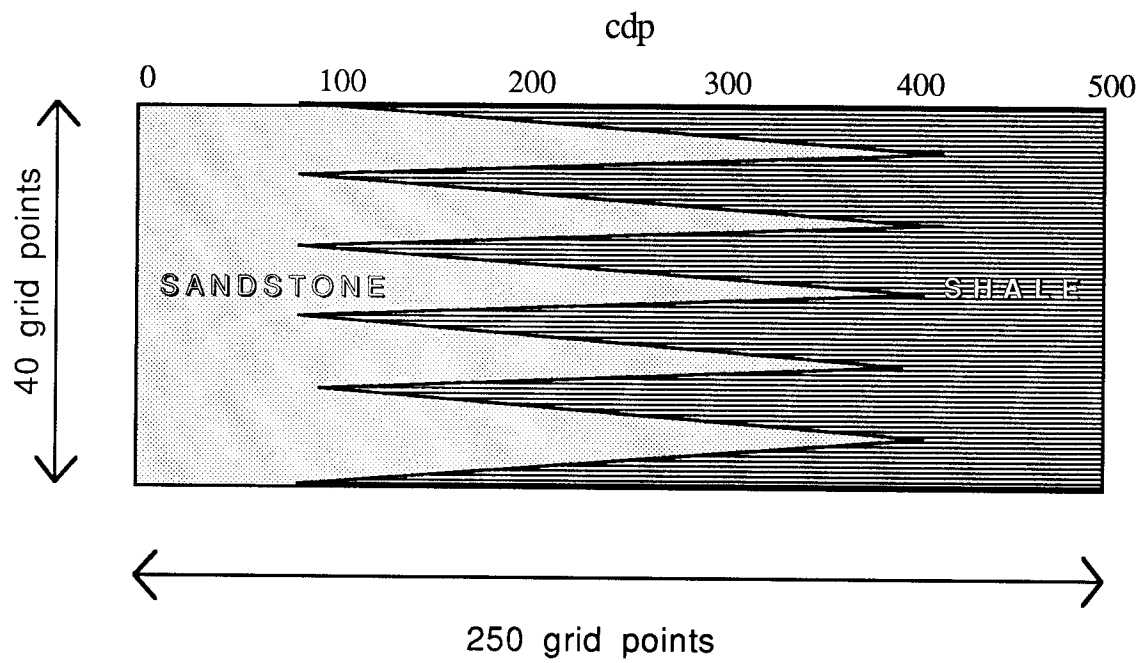

FIG. 4. Schematic diagram of the model

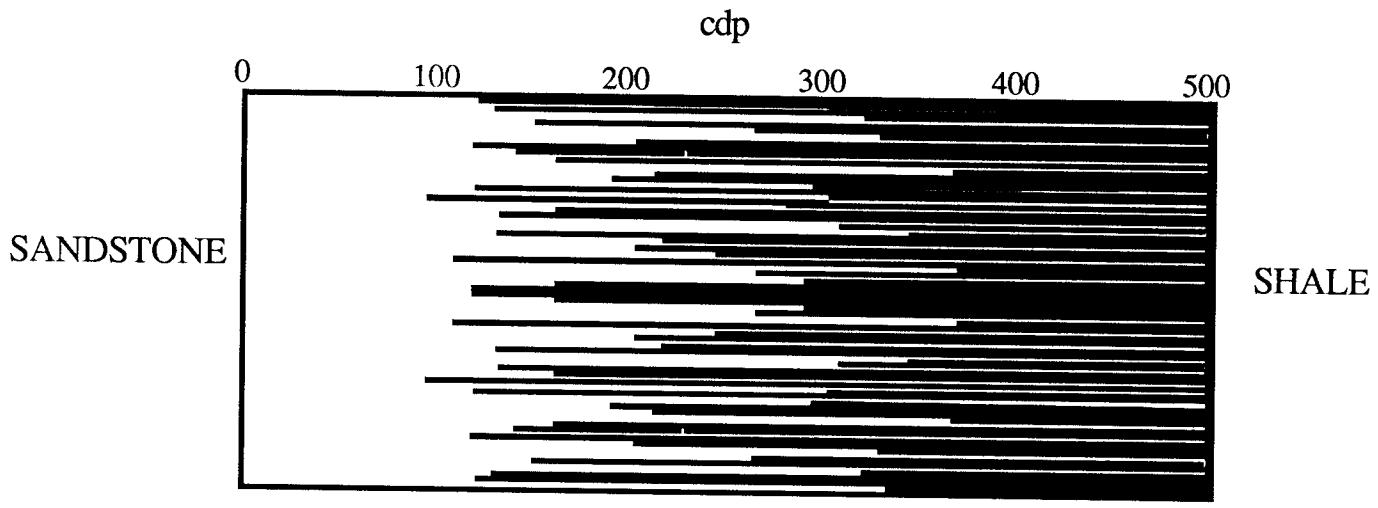

FIG. 5. A slightly more realistic picture

shot gathers

John Etgen's elastic finite difference modeling program was used to create synthetic shot gathers over the model. The model had 250 grid points in x and 30 in z. Shots were positioned at every grid point from 50 to 200. Each shot had 101 traces extending for 50 grid points each side of the shot position. Figure 6 shows the horizontal and vertical component shot gathers at grid point 100. The P-P , P-S/S-P and S-S reflections can be clearly seen. The NMO of the P-P wave reflections is symmetric but there is a marked asymmetry in the S-S reflections caused by the laterally changing anisotropy. Figure 7 shows a selection of shot gathers across the survey the change in S-S reflection NMO can clearly be seen as the elastic parameters change from those of sandstone to shale.

cmp gathers

Figure 8 shows a selection of horizontal component common midpoint gathers from the experiment. The NMO on the CMP gathers is symmetrical and for the P-P reflections it does not appear to change along the line. However the S-S reflections show a clear decrease in NMO as the CMP position moves from above the sandstone to above the shale. Note however that the apex of the S-S reflections is at the same time for all the cmps . This indicates that the vertical S-wave velocity is the same at all points across the section.

hyperbolic velocity analysis

Figure 9 shows a hyperbolic NMO velocity analysis at CMP 150 from the horizontal component data. Five main events can be seen corresponding to the P-P reflection , S-P & P-S reflections , S-S reflections, P-P and P-S-P multiples. Figure 10 shows six hyperbolic NMO velocity analyses of the horizontal component data. They show the change in S-S reflection NMO velocity but little change in P-P reflection NMO velocity. This is because the NMO is controlled by the horizontal wave propagation velocities. There is little change in the P-wave velocity moving from the sandstone to the shale but a significant change in the horizontally traveling S-wave velocity. If these velocities are used for imaging in depth a false image will be created . The P-wave section will show a flat reflector but the S-wave section will show a dipping reflector.

ACKNOWLEDGEMENTS

I would like to thank Francis Muir and Joe Dellinger for many useful discussions and suggestions, and John Etgen for the finite difference modeling code I used.

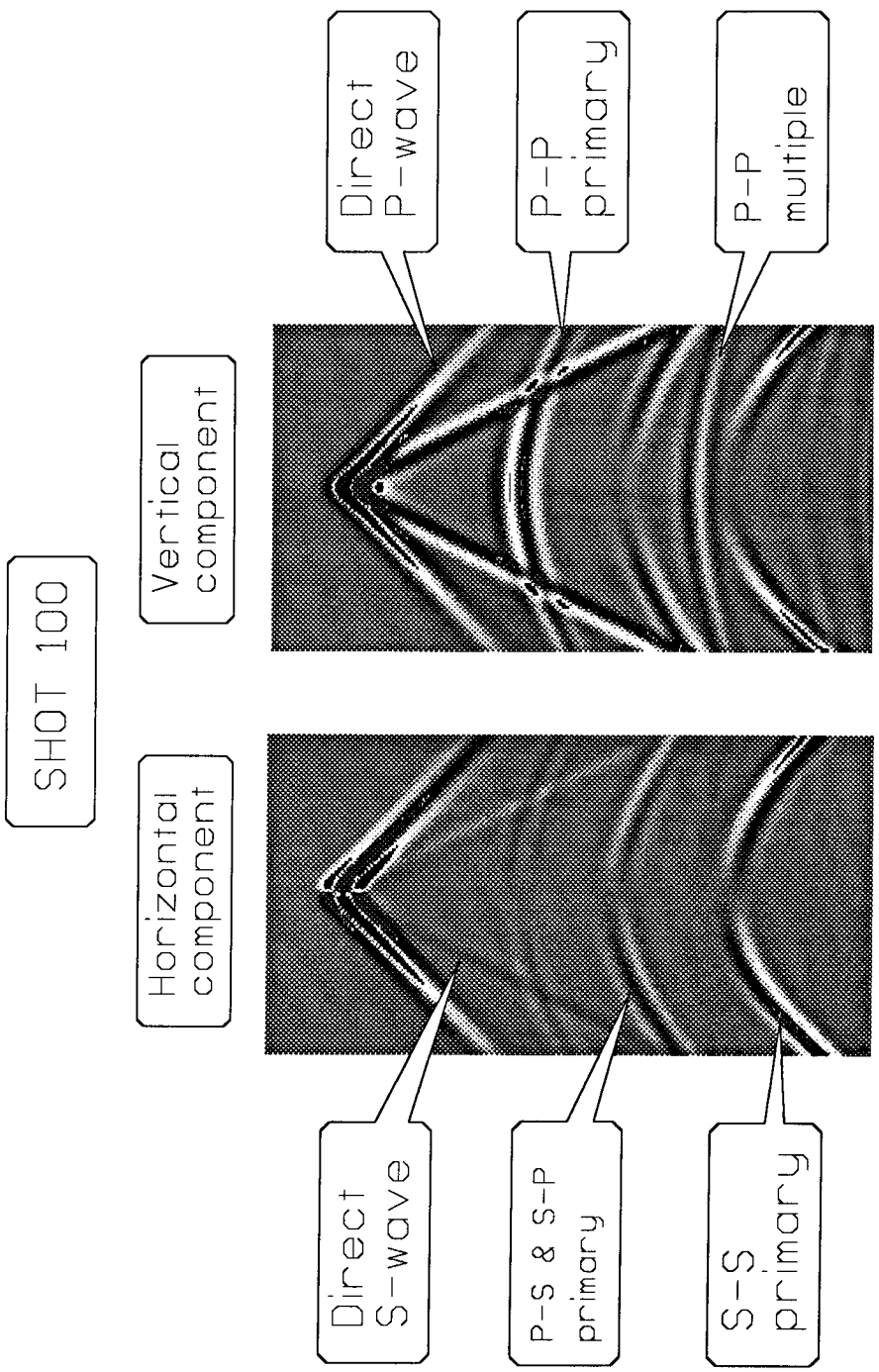

FIG. 6. Horizontal and vertical component shot gathers'

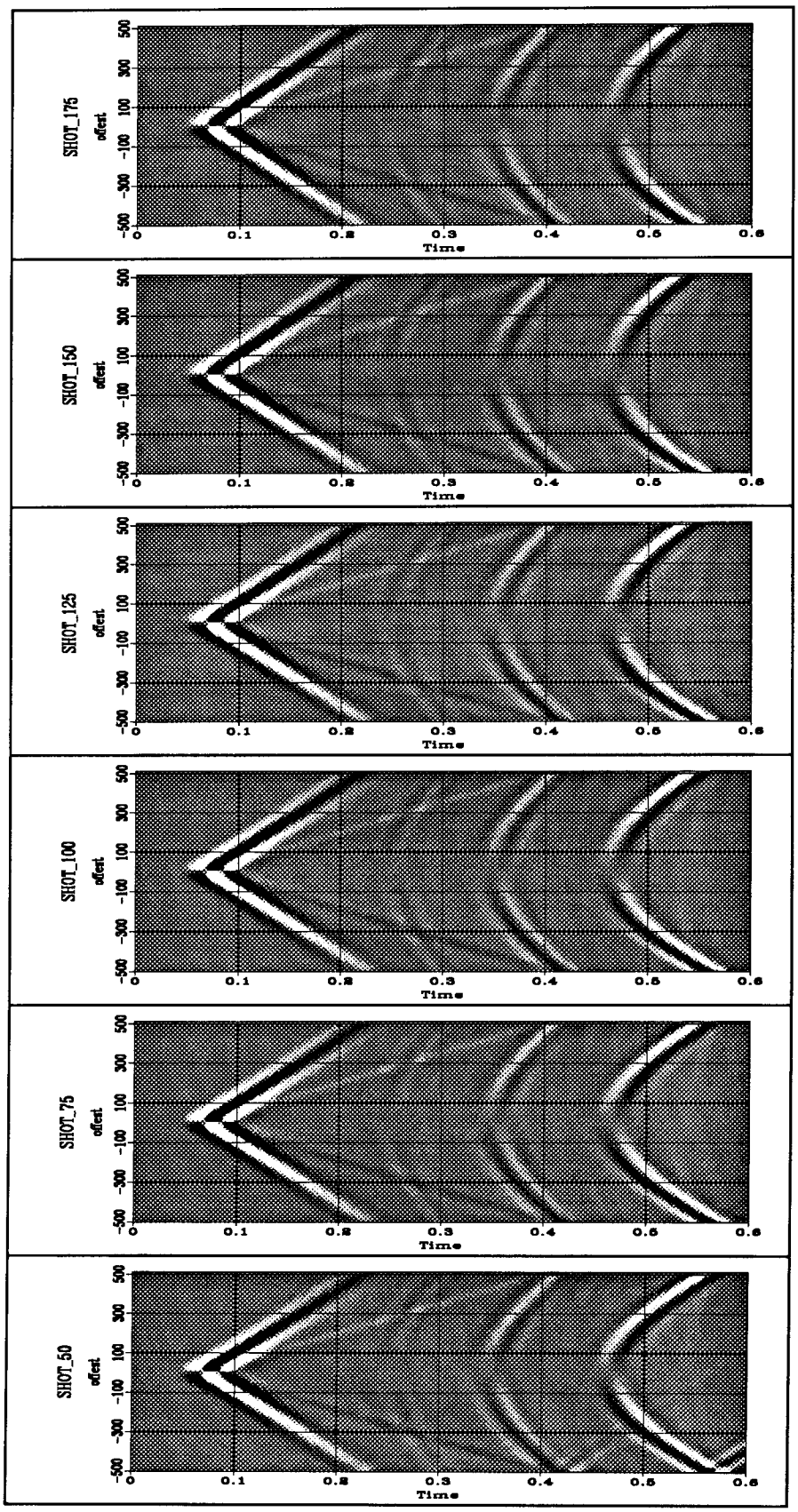

FIG. 7. Selection of horizontal component shot gathers

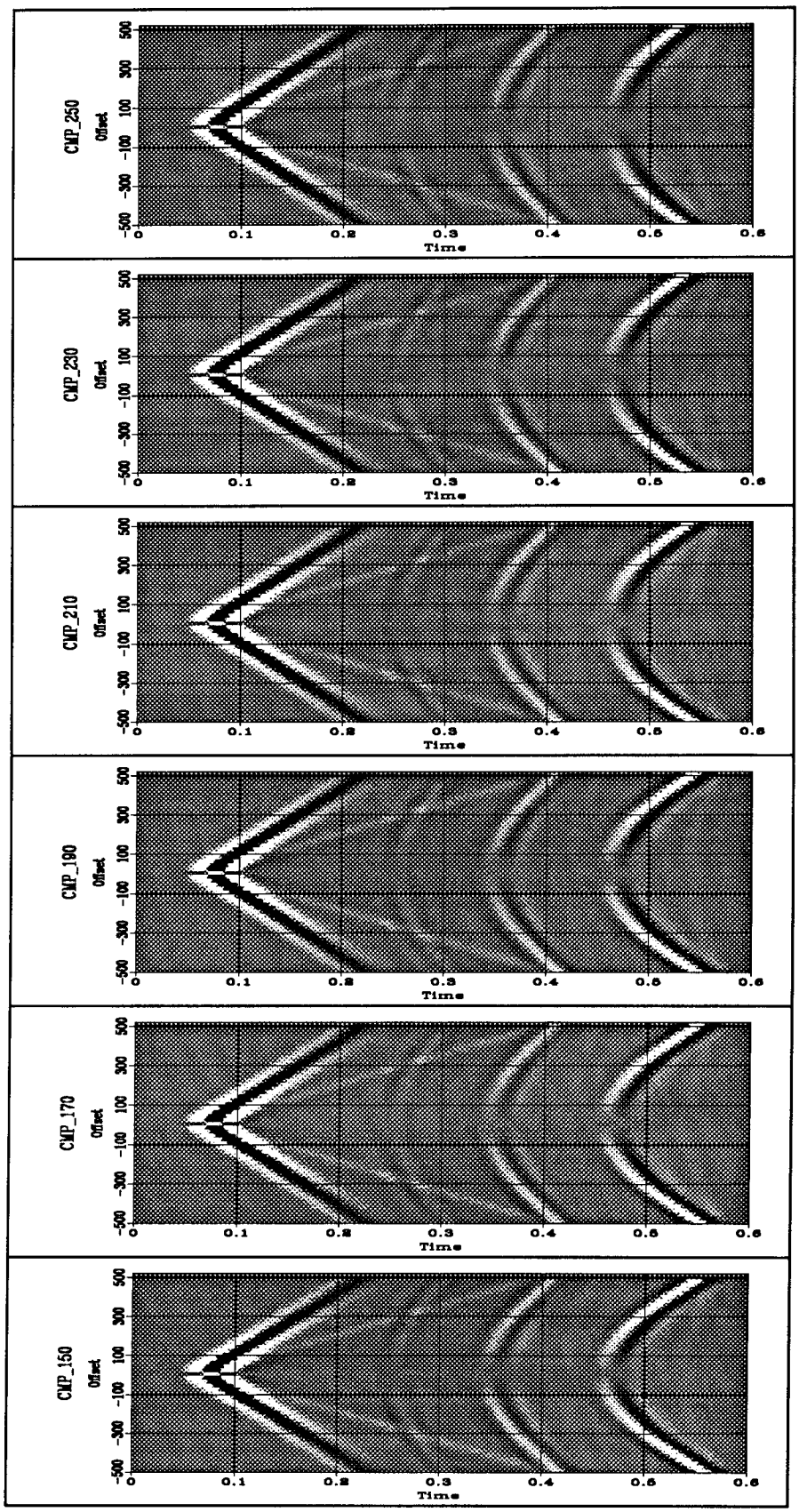

FIG. 8. Selection of horizontal component common midpoint gathers

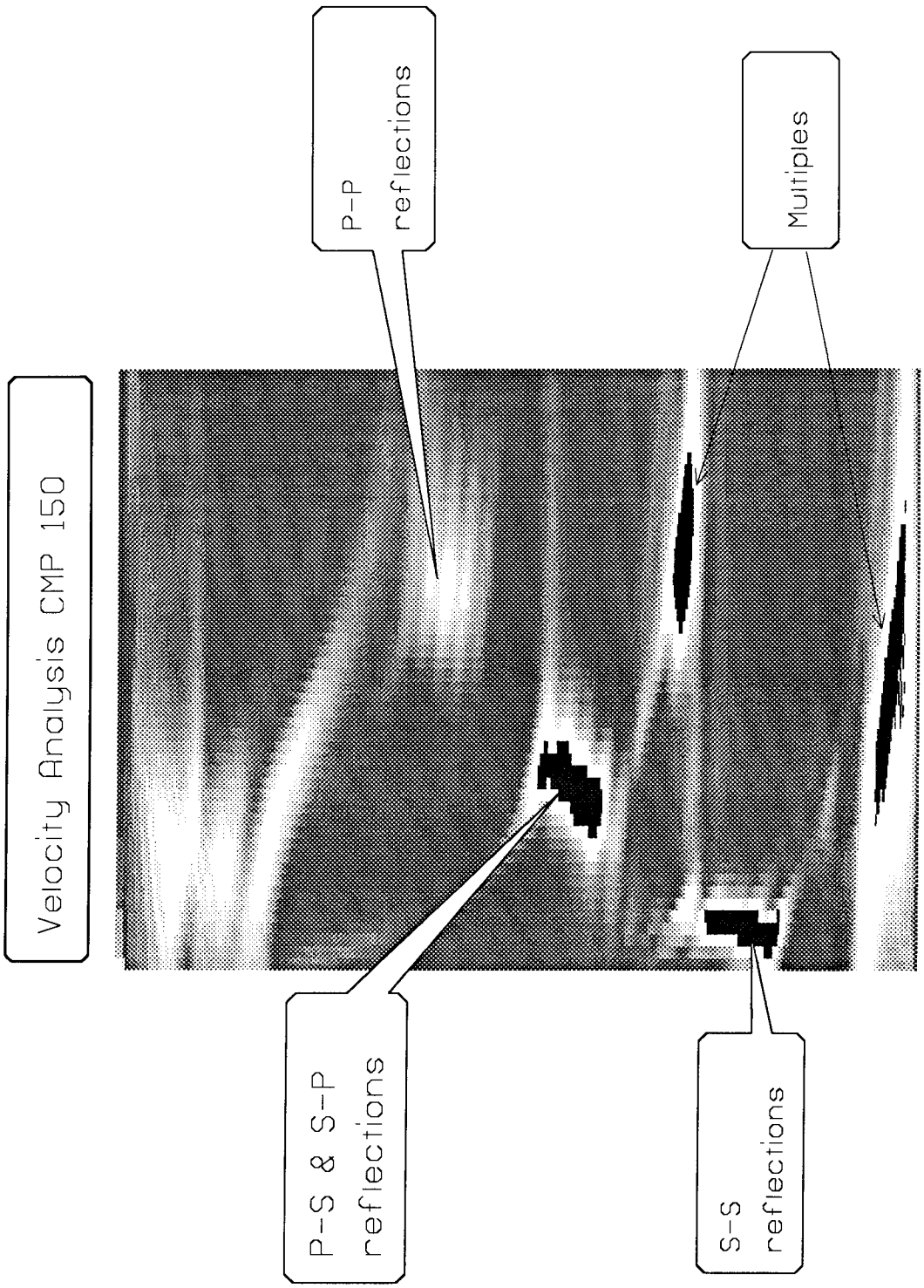

FIG. 9. NMO velocity analysis at CMP 150

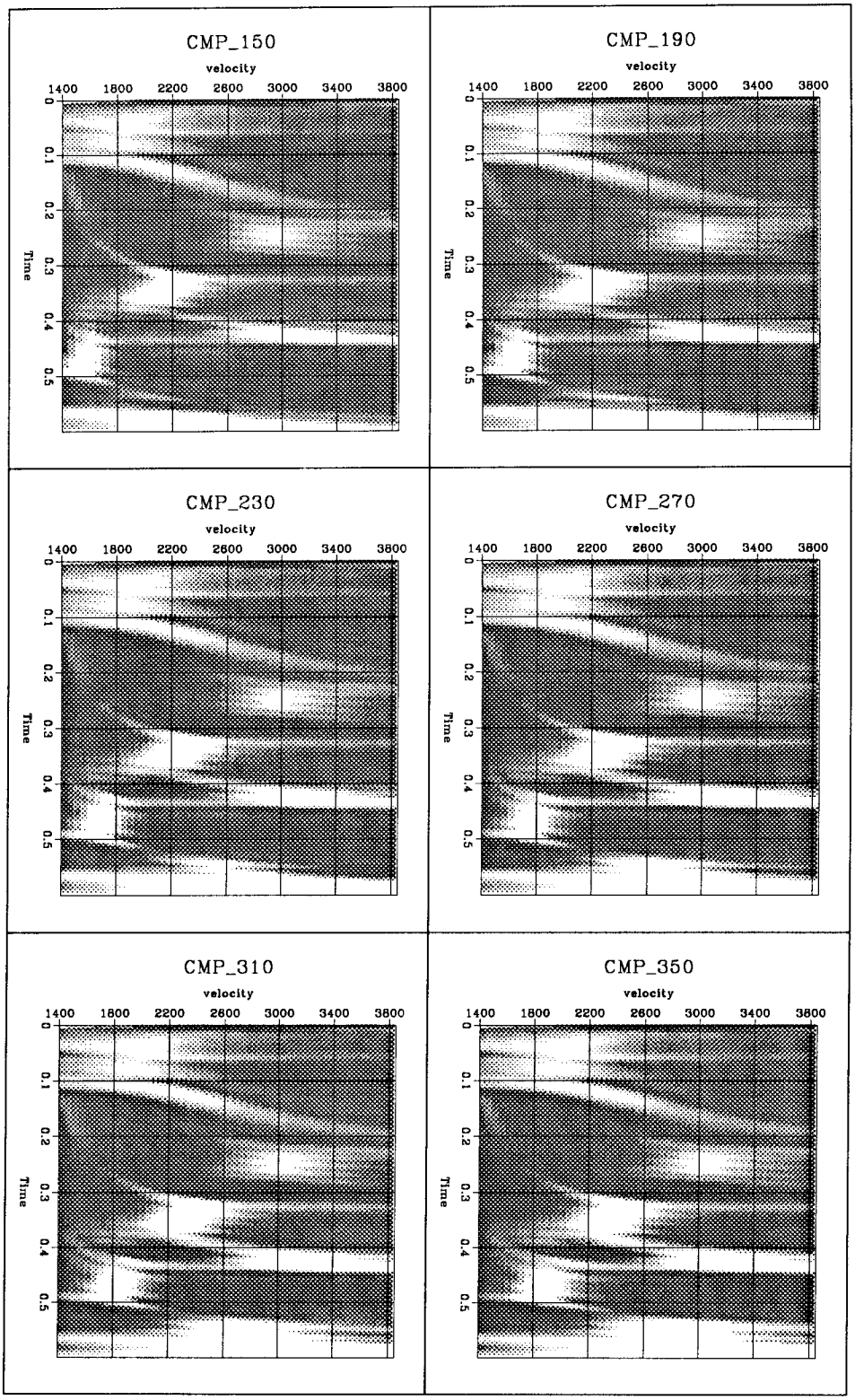

FIG. 10. Selection of horizontal component NMO velocity analyses

REFERENCES

Backus, G.E. , 1962, Long-wave anisotropy produced by horizontal layering; JGR **66**, 4427-4440.

Dellinger, J. and Muir, F. , 1985, Axisymmetric Anisotropy I: Kinematics; SEP–**44**, 1-23.

Etgen, J., 1987, Finite difference elastic anisotropic wave propagation; SEP–**56**, 23-57.

Muir, F. , 1987, Layered models, equivalence & abelian groups; SEP–**56**, 59-69.

Muir, F. , 1988, A calculus for fine layered anisotropic media; SEP–**57**.

Schoenberg, M. and Douma, J., 1988, Elastic wave propagation in media with parallel fractures and aligned cracks; Geophys. Prosp., to appear

Schoenberg, M. and Muir, F., 1988, A calculus for finely layered anisotropic media; Submitted to Geophysics.

Антигуманная идеология современного капитализма наносит все больший ущерб духовному миру людей.

–Из Программы КПСС

The anti-human ideology of contemporary capitalism causes more and more damage to people's spiritual world.
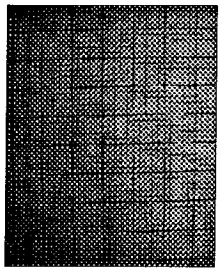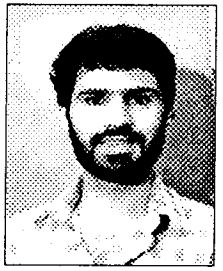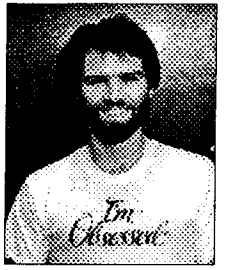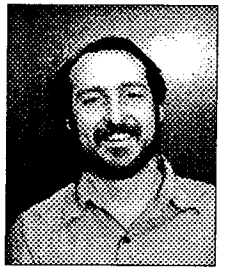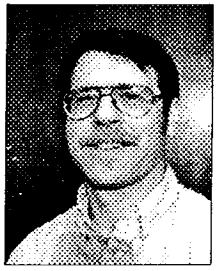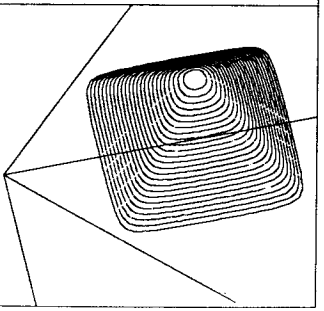
–From the Program of the CPSU